Research Article

Yuan Li, Junhong Su*, Junqi Xu, and Guoliang Yang

Characterization of damage morphology of structural SiO_2 film induced by nanosecond pulsed laser

https://doi.org/10.1515/phys-2022-0060
received February 17, 2022; accepted June 20, 2022

Abstract: We investigated the damage morphology of porous silicon oxide film with a periodic hexagonal hole array irradiated by nanosecond pulsed laser, both experimentally and numerically. To understand the damage morphology, the temperature field distribution and the thermal stress distribution during the laser radiation process were investigated by finite element method. The simulation results show that the thermal stress regulated by periodic structural surface is the reason for the circumferential and discrete distribution of the damage points. The results provide ideas for improving the laser damage resistance of the structural surfaces.

Keywords: anti-reflection, laser damage, surface morphology, periodic porous surface, temperature field distribution, thermal stress field distribution

1 Introduction

The structural surface has good optical anti-reflection (AR) properties, and the laser resistant of these optical elements is more than twice as that of traditional AR thin film [1–3]. However, it is very important to understand the laser damage mechanism of the structured surface for both laser science and its applications in high power laser systems [4–7].

Ying *et al.* [2] found that the laser-induced damage thresholds (LIDTs) of porous nanostructures on BK7 are much higher than those of AR-coated glasses. To understand the possible damage mechanisms, the role of electric field distribution inside the porous structure during the laser radiation process was investigated. They found that the temperature distribution resulting from the internal electric field may be a main factor. Li *et al.* [8] observed a slightly higher LIDT in ordered porous silica coating than in the disordered one, and the authors believe that the ordered structure is the key to interpret the high LIDT. Pan *et al.* [9] studied the laser damage behavior of three-dimensional photonic crystals with an opal structure and disordered film. The results show that the higher energy absorption and temperature rise caused by the electric field enhancement in disordered film are the reasons for the lower LIDT. So far, the mechanism of laser damage to the structural surface has not been completely understood because of the complexity of the mechanism and the diversity of structures.

The LIDTs of the samples were measured by zero probability damage criterion. The criterion of zero probability damage represents the laser energy density when the sample is critically damaged, which is the maximum energy density of the sample without damage, or the minimum energy density of the sample with damage. In this work, finite element method (FEM) was applied to simulate the distribution of laser-induced thermal stresses and temperature in periodic and porous SiO_2 film by the energy density near the zero probability of damage. The laser-induced damage morphology is discussed.

* **Corresponding author: Junhong Su,** School of Photoelectrical Engineering, Xi'an Technological University, Xi'an 710021, China, e-mail: sujhong@126.com
Yuan Li: School of Photoelectrical Engineering, Xi'an Technological University, Xi'an 710021, China, e-mail: l1802215@126.com
Junqi Xu: School of Photoelectrical Engineering, Xi'an Technological University, Xi'an 710021, China, e-mail: jqxu2210@163.com
Guoliang Yang: School of Photoelectrical Engineering, Xi'an Technological University, Xi'an 710021, China, e-mail: yangguoliang@xatu.edu.cn

2 Materials and methods

2.1 Periodic and porous structural SiO_2 film

An 800 nm SiO_2 film is grown on a 6 inch quartz wafer with plasma-enhanced chemical vapor deposition technology. Only the top SiO_2 film layer etched into the porous and

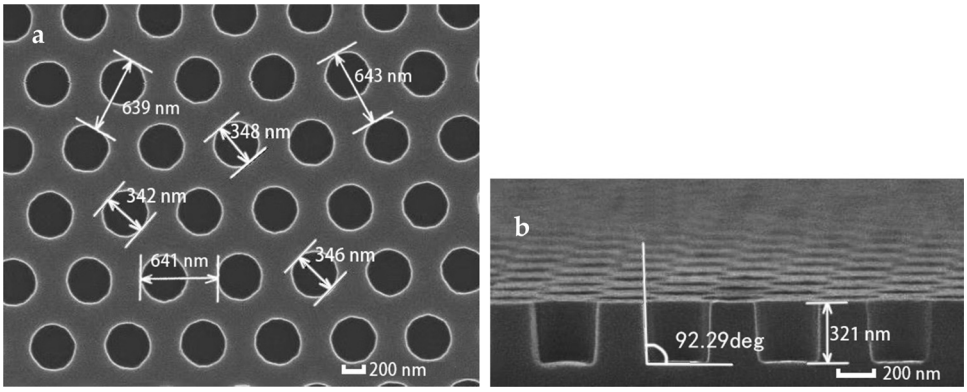

Figure 1: (a) Overhead and (b) cross-sectional SEM micrographs of nanopore arrays.

periodic nanopore arrays. Periodic hexagonal pore arrays were prepared on the SiO_2 film using nanoimprint lithography combined with ICP-RIE technology. The periodic nanopore arrays have an average diameter of 345 nm, an average period of 642 nm, and a hole depth of 321 nm; a magnified SEM image is also shown in Figure 1. The error of the fabrication is 6 nm. A typical perpendicularity of the hole wall is 92.29°.

2.2 Laser irradiation experiment

To study the mechanism of the laser damage of the structural SiO_2 film, the surface was irradiated by a single-pulsed laser. The experiments were performed in the "1-on-1" regime according to the ISO 21254 standard [10]. The scheme of the testing system is shown in Figure 2. The damage testing system is based on a Q-switched Nd:YGA laser system with a wavelength of 1,064 nm and pulse length of 10 ns. The laser beam passes through a laser-beam extender system and an attenuator to obtain the required energy. The laser beam is split into a reference beam and a probe beam by the beam splitter 1. One of the probe lights is then focused onto the sample. The second one enters the beam analyzer. The light source is used to provide a suitable ambient light. CCD and probes are used to obtain the information of the sample damage. The laser, a beam expanding system, attenuator, beam splitters, energy meter, focusing system, beam analyzer, detector, CCD, and sample gripper are all controlled by a computer program. The laser is focused on a spot with a diameter of 800 μm on the sample surface.

2.3 Simulation of pulsed laser irradiation

The damage morphology is related to the material properties and the energy density, pulse width, and the wavelength of the incident laser [11]. In order to reduce the cost of calculation, a smaller spot area of the incident laser with the same conditions as the test environment such as the energy density, pulse width, and wavelength of the laser, is used in the simulation. To understand the characterization of damage formation, a numerical simulation model is used to simulate the propagation of a single pulse nanosecond laser inside the structural film. Because the size of the laser spot used in the test is very large compared with the size of the hole, in order to reduce the cost of calculation, the same laser energy density in the test is used for the simulation, so that a smaller spot size can be used in the simulation calculation. Figure 3 shows the schematic drawing of structural SiO_2 film irradiated by a Gaussian beam. The hole period, diameter,

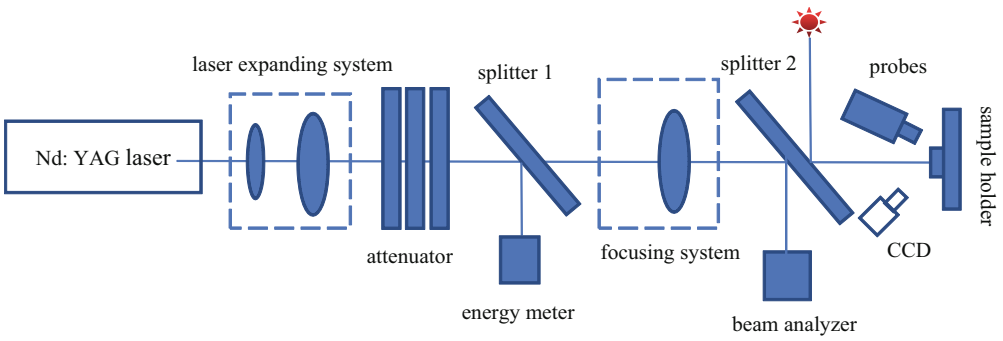

Figure 2: The scheme of the LIDT testing system for optical elements.

and depth of the structural film are 560, 345, and 321 nm, respectively. When a nanosecond laser is incident on the structured surface of the silicon oxide film, some of the energy is absorbed by the material, and the heat conduction equations before and after the melting temperature are as follows:

$$\rho c_p \frac{\partial T}{\partial t} + \rho c_p \boldsymbol{u} \cdot \nabla \boldsymbol{T} + \nabla \cdot \boldsymbol{q} = Q_{\text{ted}}, \tag{1}$$

$$\rho c_p \frac{\partial T}{\partial t} + \rho c_p \boldsymbol{u} \cdot \nabla \boldsymbol{T} + \nabla \cdot \boldsymbol{q} + Q_m = Q_{\text{ted}}, \tag{2}$$

$$\boldsymbol{q} = -k \cdot \Delta T, \tag{3}$$

where ρ is the density of the material; c_p is the heat capacity of the material; T is the absolute temperature; q is the energy of pulsed laser irradiation on the structural surface; k is the thermal conductivity of the material; u is the melting rate of materials using momentum conservation equation; Q_{ted} stands for thermal elastic damping term; and Q_m is the latent heat associated to the transition from solid to fluid phase.

$$Q_m = \frac{\rho c_p}{k} L_m f \frac{\partial T}{\partial t}, \tag{4}$$

where L_m is the latent heat of quartz glass melting; f represents the physical state of the material: when $f = 0$, it means the material is solid; when $f = 1$, the material is liquid. The laser beam was defined as a surface heat source with Gaussian distribution as shown below:

$$Q(r, t) = f_s(x, y)\, g(t), \tag{5}$$

$$f_s(x, y) = (2P/\pi r_0^2) \exp\left(-\frac{2(x^2 + y^2)}{r_0}\right), \tag{6}$$

$$g(t) = \exp(-t^2/\tau^2), \tag{7}$$

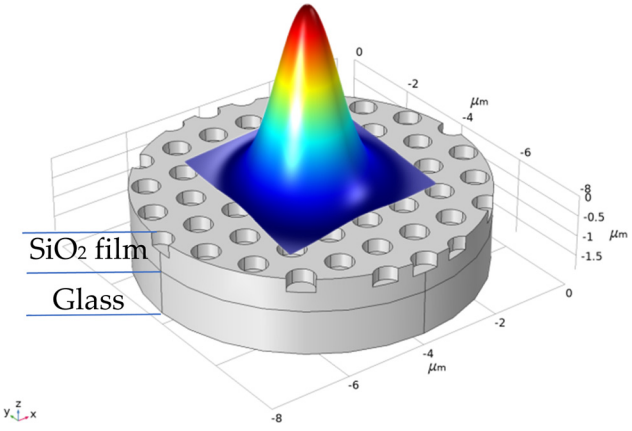

Figure 3: Schematic diagram of the geometrical model irradiated by a Gaussian beam.

Table 1: Summary of parameters used for calculations and analysis [12]

Materials	Glass	SiO_2
Melting point (K)	1,673	1,973
Tensile strength (MPa)	28	110
Compressive strength (MPa)	650	1,500
Refractive index	1.52	1.465
Absorption coefficient (m^{-1})	1.181	141.726
Specific heat [J/(kg K)]	858	841
Thermal conductivity [W/(m K)]	1.5	1.19
Young's modulus (GPa)	81	87
Poisson ratio	0.208	0.16
Linear expansibility (K^{-1})	7.1×10^{-6}	0.5×10^{-6}
Density (kg/m^3)	2,510	2,500
Lm (J/kg)	1.23×10^5	—

where $f_s(x,y)$ is the spatial distribution function of pulsed laser; $g(t)$ is the time distribution function of the pulsed laser; p is the peak power of a Gaussian beam; r_O is the spot radius of a Gaussian beam; τ is the pulse width of the laser. Table 1 shows the summary of parameters used for calculations and analysis.

The boundary condition of the structural surfaces is as follows:

$$\boldsymbol{q} = -k\nabla T = Q - h(T - T_{\text{amb}}), \tag{8}$$

where Q is the total heat source of laser irradiation; h is the convective coefficient between the surface and the environment; and T_{amb} is the ambient temperature.

Other boundary conditions are as follows,

$$-n \cdot q = 0, \tag{9}$$

where n represents the normal vector of the boundary surface.

The initial condition is as follows,

$$T(x, y, z, t)|_{t=0} = 293.15\ \text{K}. \tag{10}$$

The uneven distribution of thermal field on the structured surface leads to the distribution of thermal stress field. Then, the thermal stress is coupled with the heat conduction equation by the melting rate equation. Hooke's law is used to connect elastic strain and stress tension for linear elastic materials, and the movement equation of material deformation displacement is as follows:

$$\rho_0 \frac{\partial^2 \boldsymbol{u}}{\partial t^2} = F_V - \nabla \cdot \sigma, \tag{11}$$

$$\sigma = \sigma_{ad} + C : (\varepsilon - \varepsilon_{\text{inel}}), \tag{12}$$

where, F_v represents volume force vector; σ stands for stress tensor; σ_{ad} is the additional contribution of initial stress and viscoelastic stress; C is the elastic tensor of the

fourth order; ":" stands for the double dot tensor product (or double contraction); ε is the total strain; and ε_{inel} is the inelastic strain. These involve components of the coordinate axes.

The elastic thermal strain equation is as follows:

$$\varepsilon = \alpha(T - T_{ref}), \tag{13}$$

where T_{ref} is the reference temperature, and α is the coefficient of thermal expansion.

To reduce the computational cost of simulation, the distribution of temperature field and thermal stress field of the damaged spot were simulated under the same energy density as the experiment.

2.4 Measurement and characterization methods

A polarized light microscope (LEICADM2500P + 7HMS_0304012401, Germany) was used to observe the damage morphology of the structured film.

3 Results and discussion

The LIDT of the structural silicon oxide film with hexagonal period has been measurement in our previous work [13,14]. Figure 4 shows the LIDT test result of the sample. The laser-induced damage threshold (LIDT) of the sample is 17.6 J/cm^2. The damage morphology in Figure 5 is formed under the laser energy density of 22.3 J/cm^2. It is not difficult to see that the diameter of the damaged area is close to the spot. There are more damage spots in the periphery and the circumferential distribution is close to the diameter of the laser spot. The damage points are distributed discretely, and the diameter of the peripheral

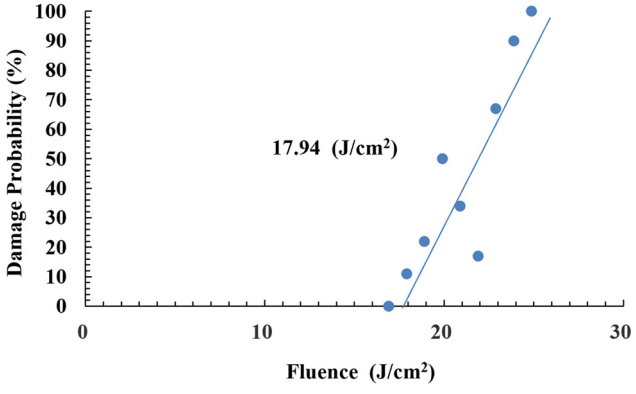

Figure 4: The result of laser-induced damage threshold.

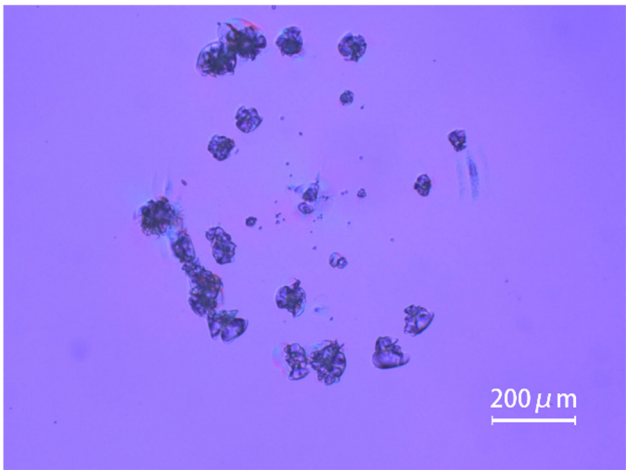

Figure 5: Damage morphology of the structural surface obtained by Polarized Light Microscopy.

damage points is larger than that of the central area. In order to speed up the calculations, these simulations were obtained for a small region. The spot and the size of the model are scaled in the same proportion. For the simplified model, 6.3 ns is the maximum temperature and the maximum thermal stress moments during the laser action time. Figure 6 shows the simulation results of three-dimensional numerical simulation under the irradiation of the laser critical energy density of 22.3 J/cm^2 at 6.3 ns. Figure 6(a) shows the isobolograms of the maximum thermal stress during laser action time. Figure 6(b) shows the maximum temperature distribution during laser action time. Figure 6(c) shows a deformation diagram of the maximum thermal stress.

Figure 5 shows that the distribution of damage points is discrete at the edge of the spot under low energy density laser irradiation, and the diameter of damage points at the center is smaller than that at the edge. Figure 6(b) shows the three-dimensional distribution diagram of the temperature field, it can be seen that the temperature in the central region of laser irradiation is higher than the temperature in the edge region. The maximum temperature in the central region is 1,660 K, which is lesser than the melting temperature of silicon oxide film (1,973 K). The stress concentration caused by temperature mutation is easy to form at the edge of spot irradiation. Figure 6(c) shows the deformation of stress, the deformation factor is 800. The upper surface exhibits tensile stress. It can be seen from the damaged morphology that the diameter of holes in the central area becomes smaller due to the tensile stress at the upper surface. The simulation results are consistent with the damage morphology. The tensile stress of SiO_2 is 110 MPa [11]. It can be seen from Figure 6(a), the red circle contour lines represent the stress values between

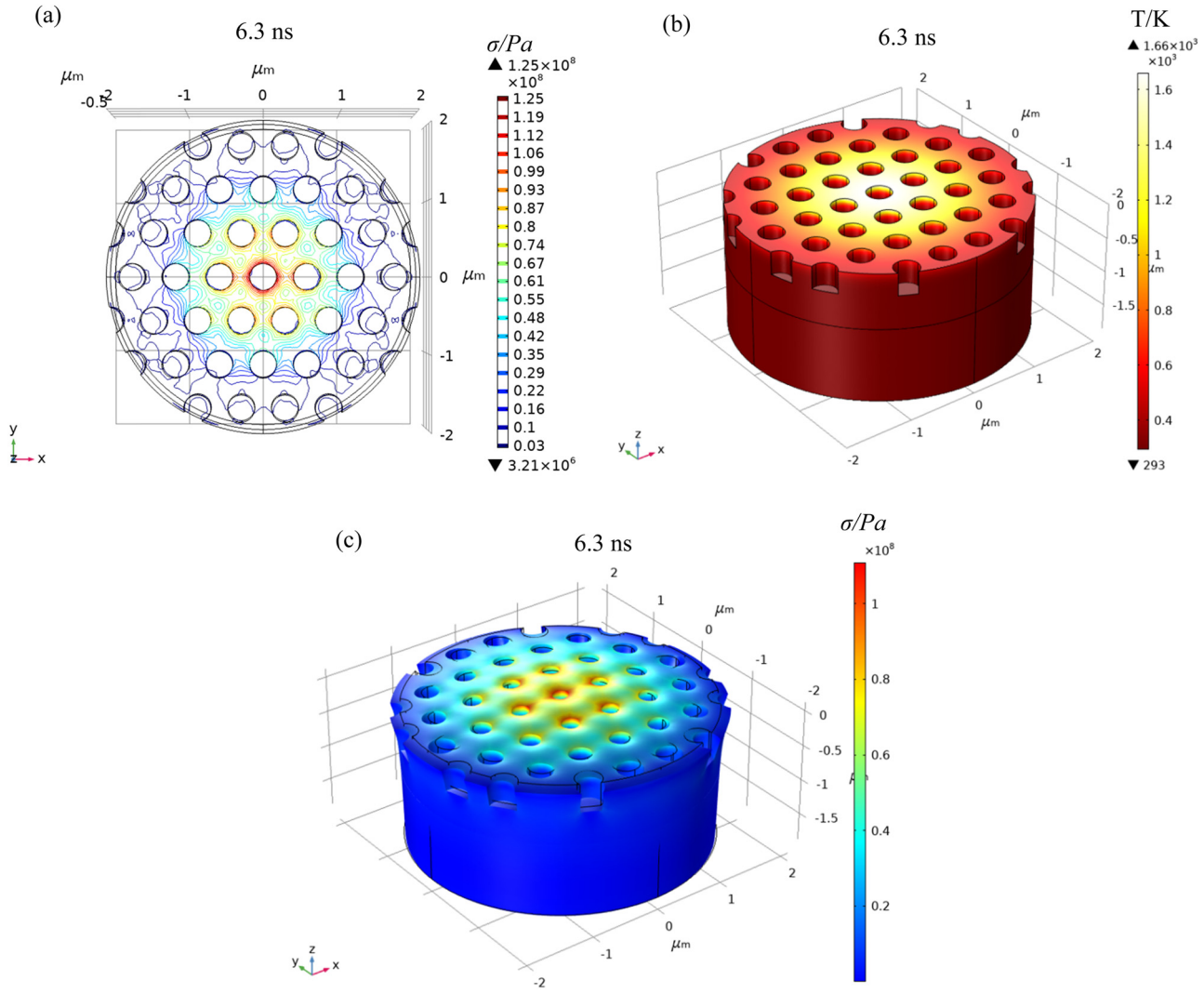

Figure 6: Three-dimensional and instantaneous simulation results under the irradiation of the laser critical energy density at 6.3 ns; (a) the isobologram of the maximum thermal stress at 6.3 ns; (b) the maximum temperature distribution at 6.3 ns; (c) deformation diagram of the maximum thermal stress at 6.3 ns.

98×10^6 Pa and 125×10^6 Pa. It can be seen that the maximum thermal stress exceeds the damage stress of the SiO_2 film. The results are consistent with the actual damage morphology, which presents circumferential scattered breaking points. So, laser-induced damage morphology of silicon oxide thin films with periodic and porous structure is due to the thermal stress distribution caused by periodic distribution of pores.

4 Conclusion

The phenomenon of discrete and circumferential distribution of damage points was found and explained. The thermodynamic process of silica thin films with periodic and porous structure irradiated by 1,064 nm laser with low energy density was investigated by FEM. The simulation results were in good agreement with the damage morphology. The simulation results show that the regulation of the thermal stress field caused by the structured surface with periodic pore distribution is the reason for forming damage points with discrete and circumferential distribution. The findings of this study will contribute to understanding of the formation mechanism of laser damage on the structural film.

Acknowledgments: The authors thank Prof. Lihong Yang for the inspiring discussion on the model.

Funding information: This research was funded by National Natural Science Foundation of China (No. 61378050).

Author contributions: Conceptualization: J.S. and J.X.; methodology: J.S. and G.Y.; experimental validation: G.Y.; simulation: Y.L.; original draft preparation: Y.L.; review and editing: Y.L., J.S., and G.Y. All authors have accepted responsibility for the entire content of this manuscript and approved its submission.

Conflicts of interest: The authors state no conflict of interest.

References

[1] Lynda EB, Catalin MF, Jesse AF, Brandon LS, Ishwar DA, Menelaos KP, et al. Anti-reflective surface structures for spinel ceramics and fused silica windows, lenses and optical fibers. Optical Mater Exp. 2014;4(12):2504–15.

[2] Ying D, Shi JL, Hong BH, Yun XJ, Fan YK, He YG. Laser-induced damage properties of antireflective porous glasses. Opt Commun. 2012;285:5512–8.

[3] Teng ZQ, Sun Y, Kong FY, Jin YX, Liu YC, Wang YL, et al. Sub-wavelength microstructures on lithium triborate surface with high transmittance and laser-induced damage threshold at 1,064 nm. Opt Laser Technol. 2022;145:107487.

[4] Manenkov AA. Fundamental mechanisms of laser-induced damage in optical materials: today's state of understanding and problems. Opt Eng. 2014;53:e010901.

[5] Ye X, Jiang XD, Huang J, Sun LX, Geng F, Yi Z, et al. Subwavelength structures for high power laser antireflection application on fused silica by one-step reactive ion etching. Opt Lasers Eng. 2016;78:48–54.

[6] Schulze M, Damm M, Helgert M, Kley EB, Nolte S, Tünnermann A. Durability of stochastic antireflective structures–analyses on damage thresholds and adsorbate elimination. Opt Exp. 2012;20:18348–55.

[7] Lynda EB, Jesse AF, Shaw LB, Ishwar DA, Jasbinder SS. Review of antireflective surface structures on laser optics and windows. Appl Opt. 2015;54:F303–9.

[8] Li X, Zou L, Wu G, Shen J. Laser-induced damage on ordered and amorphous sol-gel silica coatings. Opt Mater Exp. 2014;4:2478–83.

[9] Pan L, Xu HB, Lv RZ, Qiu J, Zhao JP, Li Y. Laser damage resistance of polystyrene opal photonic crystals. Sci Rep. 2018;8:4523.

[10] ISO Standard 21254. Lasers and laser-related equipment: test methods for laser-induced damage threshold. Switzerland: ISO; 2011.

[11] Rudolph W. Encyclopedia of modern optics. Laser-Induced Damage Optical Mater. 2018;4:302–9. doi: 10.1016/B978-0-12-803581-8.09451-0.

[12] Wang B, Qin Y, Ni XW, Shen ZH, Lu J. Effect of defects on long-pulse laser-induced damage of two kinds of optical thin films. Appl Opt. 2010;49:5537–44.

[13] Li Y, Su J, Xu J, Yang L, Yang G. Optical and laser-induced damage characterization of porous structural silicon oxide film with hexagonal period by nanoimprint lithography. Coatings. 2022;12:351.

[14] Li Y, Su J, Xu J, Yang, L, Yang G. Fitting model of laser-induced damage threshold for optical elements with periodic surface. Laser Optoelectron Prog. 2022;59(23):2320001.